Received: 7 July 2023 | Revised: 23 August 2023 | Accepted: 28 August 2023 | Published online: 31 August 2023

RESEARCH ARTICLE

Archives of Advanced Engineering Science
2023, Vol. 1(1) 38–54
DOI: 10.47852/bonviewAAES32021330

BON VIEW PUBLISHING

Estimating Maximum Power from Wind Turbines with a Simple Newtonian Approach

Ivan R. Kennedy[1,2,*], Migdat Hodzic[3], Angus N. Crossan[2], Nikolas Crossan[2], Niranjan Acharige[1] and John W. Runcie[1,4]

[1]*School of Life and Environmental Sciences, University of Sydney, Australia*

[2]*Quick Test Technologies, University of Sydney, Australia*

[3]*Faculty of Information Technologies, University Dzemal Bijedic in Mostar, Bosnia and Herzegovina*

[4]*Aquation Pty Ltd, Australia*

Abstract: Action mechanics showing torques result from rates of variation in impulsive action motivated a new method to estimate maximum power from wind turbines. Newton's third law of equality of action and reaction provides a strictly causal mechanism of wind power from the deflection of wind momentum by twice its angle (θ) of incidence on rotor blades. The transverse reaction needed to conserve deflected wind momentum provides the turning moment for turbine rotation. Action mechanics integrates impulsive wind action on turbine blades as differing torques ($\int mrvd\theta/dt \equiv mv^2$) exerted on rotor surfaces at each radius. Windward torque (T_w) is estimated from rotor dimensions, the angle of wind incidence and radial action of wind impulses on the blade surfaces (also $\int mrvd\theta/dt \equiv mv^2$). A leeward torque ($T_b$) is exerted as back reaction on turbine blades parallel to the plane of rotation of the blade. Net torque is then converted to potential power (T_w - T_b)Ω by the angular velocity (Ω) of the turbine rotors, a function of tip speed ratio to wind speed. Better predictions of limits to wind power can be made, by including control of optimal wind angle and blade length. An analysis of the equivalence of deflected air momentum on turbine blades or air foils for aircraft reveals that even the lifting action on air foils can be explained by the normal reaction to the momentum in an air stream, also deflected by an angle twice that (2θ) of incidence. Release of vortical field energy from laminar flow of air in winds as heat is predicted in turbulent wakes, possibly affecting achievement of maximum power output by wind farms. Significant heat release by downwind turbulence from vortical energy requires their careful location. Diligence demands that use of windfarms as sources of renewable energy should minimize any environmental impacts, such as drying of landscapes.

Keywords: radial action mechanics, wind power, torque, turbulent heat release, anticyclone, Penman–Monteith equation, environmental risk mitigation

1. Introduction

Applying the action principle of classical mechanics to explain potential energy for wind flows provides a novel but fundamental approach to estimate maximum power from wind turbines (Kennedy & Hodzic, 2023). Current models of wind turbine function use principles of fluid mechanics based on the continuum hypothesis (Batchelor, 1967) derived largely from airfoil and propeller theories. The Rankine–Froude momentum and actuator disk models were developed in the 19th century with Betz and later Glauert providing refinements related to wind turbine efficiency, including more recent developments (Glauert, 1935; Sørensen, 2016) referred to here as blade element momentum (BEM) theory. These models may include losses from the axial motion of the air induced by rotors, in contrast to the radial action model proposed here that assumes turbine blades generate power while rotating into undisturbed air, independent of the downwind wake.

In brief summary, BEM leads to an expression for power output (P) according to the following Equations (1) and (2) as a function of the cube of wind velocity (v), air density (ρ), the area swept (A_D) by the rotor blades with diameter D, and a specific axial induction factor (a) related to changes in angular momentum of the air flow.

$$P = 2a(1-a)^2 v^3 \rho A_D \quad (1)$$

$$P = 0.593 v^3 \rho A_D/2 \quad (2)$$

This enables power extraction for a system that includes a rotating wake, claimed to give a maximum power consistent with

*Corresponding author: Ivan Kennedy, School of Life and Environmental Sciences, University of Sydney, Australia. Email: ivan.kennedy@sydney.edu.au

the Betz limit for power from the kinetic energy of 0.593. Taken with other inefficiencies, a power output of about 30–40% of the theoretical maximum possible from estimated kinetic energy is found in practice.

By contrast, from Newton's third law of equality for action and reaction, an approach based on the angle of elastic deflection of wind momentum on turbine blades is offered, generating wind and reaction torques as rates of impulsive action on rotors, proportional to radius. Using such action mechanics to calculate power output, there is no requirement to consider induction effects on air flow after primary impacts with turbine blades. Action mechanics (Kennedy & Hodzic, 2021) has been defined using mean values for statistical variation in radial separation and temperature of molecules undergoing impulsive collisions, allowing accurate estimation of the action and entropy of atmospheric gases. In our subsequent revision of the Carnot cycle designed to predict in a reversible heat-work system maximum power from heat engines (Kennedy & Hodzic, 2023; Kennedy & Hodzic, 2021), such molecular action states were found to define the density of virtual quanta establishing a Gibbs quantum field sustaining the molecular kinetic pressure responsible for work processes on elastic surfaces. Molecular kinetic energy alone would be insufficient to explain these processes because reversing between two temperatures is a null process, even if functional. This complementary notion of the significance of the Gibbs action field challenges the widespread assumption that heat is merely molecules in motion. Further, we introduced the notion of vortical action and energy (Kennedy & Hodzic, 2023; Kennedy & Hodzic, 2021) as a function of transverse wind velocity in anticyclones and cyclones, a new concept.

The science of wind power is recognized to have challenges for application (Veers et al., 2019). An understanding of atmospheric and wind power flow physics is far from complete; currently, the mesoscale and microscale are numerically modeled in fundamentally different ways. The aerodynamics of wind turbines constantly being built larger explores new territory, increasingly above the surface layer. The systems science required for integration of wind power plants into electricity grids is still being developed. Our proposal of mesoscale vortical energy sustaining anticyclonic winds may have strong implications for new understanding since wind power is no longer based directly on kinetic energy (Kennedy & Hodzic, 2023). The impact of wind energy on insects, on spatial distribution of air velocity, temperature, moisture, and precipitation in the vicinity of wind parks with noise all attract attention that may be related to the novel mechanisms of wind power discussed in this article (Thess, & Lengsfeld, 2022). Extracting power from wind in complex terrain using actuator disk models could also benefit from better understanding of atmospheric dynamics in rougher surfaces (Elgendi et al., 2023). Experimental studies of aerodynamic performance of airfoils with surface modifications affecting elastic responses such as introducing slats need further analysis, emphasizing how important clean surfaces are (Viré et al., 2022). The current article assumes perfect elasticity in response to the action of wind power and integration of such studies with the results to be discussed here is suggested.

The scientific question asked here is whether this simpler action–reaction theory can be a more accurate way to estimate power output from wind turbines, coupling Newtonian force to action mechanics (Johnson et al., 2016), from the idea of least action initiated by Leibniz (Kennedy & Hodzic, 2023). Given Isaac Newton's youthful interest in the causal theory of windmills shown by his recently discovered inscriptions on the farmhouse walls at Woolsthorpe, this possibility seems apt. The purpose of this paper is to test this hypothesis from its predictions, allowing the exercise of Ockham's razor to judge its success. Several such predictions regarding power output will be made.

This article is structured as follows. In Section 2, the radial action mechanics theory for wind power is developed, generating the functional torque equations needed for computation of power, replacing Bernoulli's kinetic function for the axial difference in upstream and downstream flows of air in Equation (1). In Section 3, estimates of maximum power using these equations for a known range of horizontal wind turbines are given. These show that the fundamental Newtonian approach proposed seems valid, giving very acceptable results by comparison with specifications. In this article, we also demonstrate that the limits for power from wind from Bernoulli theory may have been underestimated, with its development of vortical energy as sustaining the rotational action of anticyclones and cyclones, discussed elsewhere (Kennedy & Hodzic, 2023). In future work, this may provide improved design for wind turbines and increased efficiency in harvesting power from wind farms.

Thus, the scope of this article is rather broad. Not only do we advance a simpler method to estimate wind power but we do this in the context of a possible major role of vortical energy in wind power (Kennedy & Hodzic, 2023). Unlike Bernoulli theory where kinetic energy together with its pressure alone is taken as causative, vortical energy sees torques and kinetic energy in wind as the result of impulsive action from quanta occupying a Gibbs quantum field. Furthermore, we conclude that this vortical energy causes a risk of regional heating when laminar air flow becomes turbulent, not an outcome predictable from continuum mechanics theory or its partial differential equations. In Section 4, we discuss differences between current theory and radial action, showing decisively that the latter can even be applied to air foils lifting aircraft, further validating the theory of reaction to deflected momentum as causative. Finally, possible risk of environmental effects from wind farms will be examined.

2. Methods

2.1. Radial action theory for estimating wind power

In the radial action model for estimating wind power, the details of blade aerodynamics need only be considered later as refinements. Similar to Carnot's purpose in defining cycle for heat engines (Kennedy & Hodzic, 2021) the radial action cycle for wind turbines should be considered as an ideal estimate of the maximum possible motive power. Inefficiencies from friction or other causes will not be dealt with here. Radial action mechanics should apply to rotor blades of any shape, while the fundamental differences in geometry and the torques generated by the windward [T_w] and leeward surface [T_b] must be respected. Figure 1 models the torques generated on the blade surface areas, allowing the maximum power to be estimated as a function of

Figure 1
Windward (T_w) and leeward (T_b) back torques developed on a rectangular rotor blade. Equations were generated from trials using a numerical program using dimensions shown. The theory provides a theoretical maximum of power for a given angle of wind incidence, obtained by the difference between torques T_w and T_b, occurring at a true angle of incidence as shown in θ ca. 30°

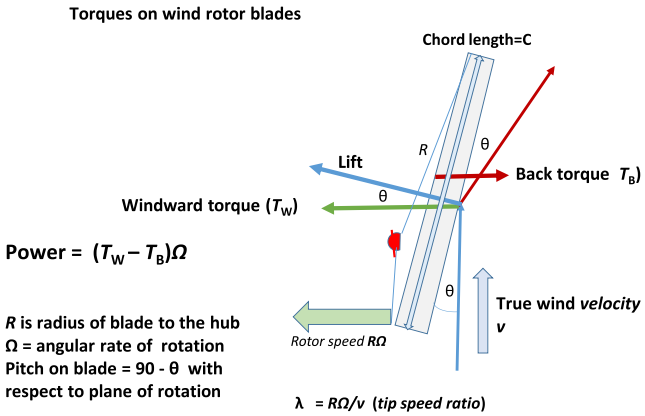

wind speed, its angle of incidence, and the actions and reactions in the blade surface material, controlled by the blade length (L or R), chord width (C), and the tip speed ratio [$L\Omega/v = \lambda$] of rotor tip speed [$L\Omega = V$) compared to wind speed [v].

The main results found from our causal analysis of the impulsive action on the windward surface of the turbine blade (Figures 1 and 2) follow. This discussion aims to justify the governing equations for radial action wind power.

(i) Impulses [$\delta mv = \delta mr\omega$] generated by oblique reflection of material particles on elastic rotor surfaces envisaged by Newton's experiments for conservation of momentum power the turbine's rotation at the hub, if free to do so. Vortical action impulses [δmvR, J.sec] with R the radial dimension to the hub reflect the momentum of wind trajectories from the surface. The rate of impulsive action [$T_w = \Sigma mvRd\theta/dt$, J or N.m] provides the magnitude of the windward torque exerted.

(ii) The angle of incidence θ is also the angle of reflection elastically from a flat surface (Figure 1), giving a total deviation angle of 2θ for the momentum. The deflected forward velocity is the source of the effective lift normal to the flat surface, balancing this angular deviation.

(iii) A turning moment and torque is exerted by the release of elastic stress within the blade material in the plane of freedom of rotation of the turbine, at an angle normal to the direction of wind incidence. The magnitude of the turning momentum [$Mv\sin2\theta$] and its cause is illustrated in Figure 2(a). Here the transverse rate of momentum from the deflection action proportional to $+Mv\sin2\theta$ and its equal and opposite reaction of $+Mv\sin2\theta$, being zero considering that there was no lateral momentum to the wind initially.

(iv) The radial action theory assumes the leading edge of the rotating blade normal to the wind is continually entering undisturbed air. The vortical stream of air effectively in laminar flow with high Reynolds number Re carries a Gibbs quantum field many times greater than the kinetic motion $\frac{1}{2}mv^2$ (Kennedy & Hodzic, 2023). The stream elastically reflected to the right in Figures 1 and 2 carries its own modified field with a cross moment normal to the wind in the plane of blade rotation of $+Mv\sin2\theta$. The decrease in the forward motion is $v(1 - \cos2\theta)$. The component of the wind velocity v with respect to the chord of the blade of $v\cos\theta$ is conserved as long as the impacts are all regarded as perfectly elastic without friction.

(v) The windward axial turning moments $+mv\sin2\theta$ exerted as torques on the turbine blade and causing its rotation are also considered as elastic. To the extent that impacts are inelastic releasing heat, a factor for the coefficient of restitution could be included, affecting the coefficient of performance C_p for power output by the turbine. The rotation velocity $R\Omega$ achieved at the points of impulse on the blade has a ratio with wind speed v of $\lambda = R\Omega/v$ with a maximum λ_L at the blade's tip speed at its length L.

(vi) This application of Newton's third law of action and equal reaction requires that the true wind direction be considered to estimate the surface reaction on the turbine blade. The apparent change of wind direction caused by the rotation of the rotors, critical in BEM theory, is irrelevant in the radial action model. Current blade momentum airfoil theory assumes lift normal to the blade and drag in the same direction as the blade; taking account of axial air motion downwind is an unnecessary confusion of cause and effect for impulsive radial action.

(vii) Two kinds of impulsive force on the blades need to be considered. The first of these is uniform with length along the blade from hub to tip reflecting windward impulses on the blades' surfaces, giving the total torque generating the rotation, proportional to radius; the second impulsive force is a Newtonian reaction torque, also variable with blade radius R from impacts by the rear of the advancing blades on air molecules, tangential to the direction of rotation (Figure 1). At tip speed to wind velocity ratios greater than one, the back torque involves impulses of greater magnitude than ever seen in airfoils unless rapidly gaining altitude.

(viii) As a result, for most of the blade, except that adjacent to the hub, no drag force operating in the wind direction can be caused by turbulence on the downwind surface given the normal reaction from air molecules to the rear of the blade; the drag on airfoils has little or no analogue in wind turbines (Figures 1 and 2). If the airfoils of aircraft are considered the same as the blades of wind turbines, the aircraft should be rotating around its longitudinal axis as it is impelled forward by propellers or the thrust of jets.

Figure 2 also compares the radial action and BEM models to explain the lift exerted on the blades of wind turbines. Radial action is clearly a more fundamental approach, based on classical mechanics of action and reaction, also separating windward and back torques as directly opposing processes. Shown in this diagram (Kennedy et al., 2021), BEM combines lift (L) and drag (D) forces to estimate the torque force (F_T) turning the rotors from a set of equations providing factors able to adjust performance to match observations. Wind speed and angle of attack in BEM are adjusted for the speed of rotor rotation ($R\Omega = V$) allowing effects of blade radius on drag to be estimated using air foil theory.

In Figure 2, highly elastic action and reaction causes stresses and strain that asymmetrically intensifies chemical potential in the rotor material, causing a windward torque (T_W) eased by freedom for rotation. By contrast, BEM is based on air foil theories of lift

Figure 2
Comparison of radial action moments (RAM) and blade element momentum (BEM) axial forces. The source of turning impulse ($-v\sin 2\theta$) is exerted from the surface normal to the wind direction (θ)

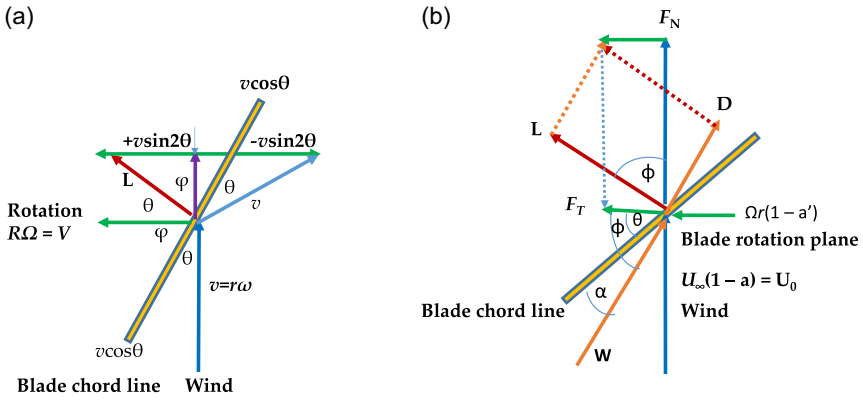

and drag exerted at right angles, adjusted for the speed of rotation of blades with radius affecting the angle of attack (α) varying with radius. Wind speed (U_∞) is also adjusted by the axial induction factor).

The introduction (Figure 2(b)) of two factors for wind speed and blade rotation, the axial induction factor (a) for the reduction in incoming wind speed (U_∞) and the tangential induction factor (a') capturing the increase in tangential velocity of the blades with radius affecting wake rotation, allows causal forces and resultant factors such as apparent change in wind speed to be included in the analysis (Johnson et al., 2016). Forces from air flow over an airfoil responding to angular dimensions of the blade are decomposed into lift and drag, normal and tangential to the apparent wind speed. This enables estimates of forces rotating the turbine and those just bending the rotor to be separated, taking the axial induction factor (a) of Equation (1) into account to estimate torques. However, we identify possible flaw in this model, caused by overestimating the interception of wind kinetic energy by the blades often only 4% of the total area. Furthermore, the analogy of turbine blades as airfoils may be inappropriate, with the description of the inertial power of wind as kinetic judged as inferior (Kennedy & Hodzic, 2023; Kennedy & Hodzic, 2021). By comparison, radial action (Figure 2(a)) is more precise in separating causes and effects, in terms of physical assumptions such as the elasticity of its action and reaction and that the vortical momentum of wind delivers impulses to the blade surfaces corresponding to its actual free velocity. The aim of this article is to test whether this simpler approach is valid. Some adjustments may still be necessary for radial action to correct for imperfection factors like inelasticity from experience in future.

2.2. Deriving equations for the rotor-turning moments from Newton's collision rule

Despite any variation in the path of individual air molecules in laminar flow near the blade surface, it is a fundamental principle of Newtonian mechanics that for a fully elastic surface the linear momentum with respect to the reflecting surface or chord is conserved. In Figure 2, we formulate our use of this principle showing the component of velocity with respect to the blade chord compared to wind velocity v at the angle of incidence θ is $v\cos\theta$, both before and after deflection from the blade. By Newton's experimental law usually given in textbooks on theoretical mechanics, the impact of elastic bodies for oblique collisions on smooth surfaces will be reflected by the same angle, for coefficients of restitution of 1.0. For smooth surfaces, there is no force parallel to the surface and the component of the particle velocity in the direction of motion is shown in Figures 1 and 2 as fully conserved with the angle of reflection equal to the angle of incidence. By claiming calculation of maximum power, we assume perfect elasticity in response. Because impulsive force is involved in the action of wind particles on blades, the principle of energy conservation is not expected to apply. However, since the deflected momentum in Figure 2 is $-M\sin 2\theta v$ an equal and opposite reaction so that overall net reverse momentum must be $+M\sin 2\theta v$, applied to the rotors free to move normal to the wind direction.

For oblique impacts in the range 0–90°, asymmetric compression of blade material at the surface is generated as an oscillating function, dependent on the elasticity and density of the blade material. If the blade surface remains clean and elastic, this variation in stress as reactive pressure produces strains distorting the windward surface, varying the chemical potential in the compressed zones as a function of the angular deviation of the reactions. As a relationship between elastic stress and strain, this reaction within the blade can be described as a function of Young's modulus (E) for the rotor surface material, with surface stress σ or uniaxial force ($m\omega^2$) and strain ϵ equal to the distortion of length ($\delta l/l$). Any departure from perfect elasticity with a coefficient of restitution less than 1.0 will diminish achievement of maximum power.

$$E = \sigma/\varepsilon \tag{3}$$

For the blade material distal to the point of wind reflection, the physical reaction to the initial radial impulses is distributed in an arc of $(90 + \theta)°$ while for the proximal reaction the arc for compression is $(90\text{-}\theta)$. The arc difference being 2θ, the turning moment per molecule on the rotor's axis is proposed to vary with $mv\sin 2\theta$ (Figures 1 and 2(a)), thus balancing action and reaction. At 90° or π/2 radians, this function becomes zero with any turning moment now symmetrical totally devoted to bending rather than turning the blade on its rotational axis at the hub. Obviously, this analysis can only be applied to compressions on the windward side of the rotor blades. The other factors determining the windward torque are the density of air (ρ), the chord width (C), and $\sin\theta$, determining the volume

and the mass of air impacting the blade per second. This represents the instantaneous force from the magnitude of momentum impacting per second for the area normal to the wind flux. When integrated with respect to the radius (R) over the entire length of the blade (L) the cumulative torque [T_w] exerted at the hub is given in Equation (4).

$$T_W = \int_0^L (\rho\delta LC sin\theta sin2\theta\ v^2 R)dR = \int_0^L (Msin2\theta\, vR/\sec)dR\ \ [\mathrm{ML^2T^{-2}}, \mathrm{J\ or\ N.m}] \quad (4)$$

This equation comprises factors for the 3-dimensional density of air (ρ), the normal area of the blade at R ($\delta RC\sin\theta$), the momentum per second [$\rho\delta RC\sin\theta v = Mv$] made normal to the wind by sinθ, and the extent of lateral reaction, thus [$Mv\sin2\theta$]. Numerically, the square of the wind velocity (v^2) is involved, one to estimate the mass of air impacting the blade per second and second to establish the magnitude of action impulse per second proportional to the variation in action (δmvR) per molecule. This is considered as involving a rectangular blade in Figure 1 but different versions of the blade area at any radius can be estimated from variations in the chord width (C) as a function of the radius to the hub (R). The 3-dimensional density is regarded as a thermodynamic function, given that wind is a cooperative action with its radial inertia involving not just the kinetic energy of molecules striking the rotors on the windward surface but with vortical energy and its resulting chemical potential. This vortical energy unique to vortexes is explained in Results and in Discussion sections. The windward torque (T_w) is predicted to be proportional to the square of the blade radius when integrated as momentum per second along the blade to L ($T_w = Mv\sin2\theta L^2/2$).

2.3. Leeward torque of rotor blades

It is said that a youthful Newton while designing his flour windmill estimated wind force by the difference between the distances he could leap with and against the wind. This image is consistent with our model of the impact of the inertia of the blade on that of air. In contrast to the windward torque [T_w] proportional to radius, in which the wind factor v^2 applies uniformly with radius R over the rotor blade from hub to tip, the back torque (T_b) varies with the square of the radius, caused by the variable rate of impacts on the air behind the blade variable with R during rotation. Given that the speed of rotation [$R\Omega$, m s^{-1}] determines both the instantaneous mass of air impacted per second and the radial momentum of these impacts, the specific action integral required is of radius squared [$R^2\Omega$]. An initial run of the model mistakenly used $R^2\Omega^2$ as a computing factor was found to produce a result with dimensions of power rather than torque. This justified integrating the specific action per radian ($R^2\Omega$) as action mechanics suggests instead of the energy per unit mass [$R^2\Omega^2$]. A variable inertial torque varying along the blade is integrated with respect to velocity and radius to provide the correct rate of impulses exerting torque.

An important difference between windward and leeward impulses with air molecules lies in the irreversible nature of impacts from the blade on air molecules. While windward impulses may be considered as a balancing of inertial forces from the wind sustained by vortical energy on the blade reaction, the leeward impacts generally exceed the wind speed except near the hub and cooperative resistance from air at the rear of the blade is much diminished and is ignored. As a result, the density of air molecules is effectively exerted from 2-dimensional action impulses exerted as a series of minute slices of air, varying with radius. If the number density of molecules in a cubic meter is taken as proportional to n^3, then n^2 must represent the density of molecules the blade encounters as a continuous process. Taking the density as having a fractional exponent, the factor required should be $\rho^{2/3}$ or 1.145 rather than 1.225. This prediction should be confirmed by experiment. By such a choice the correct physical dimensions to describe the rate of transfer of momentum from the blade to air molecules, integrated with respect to R, obtains the rate of impulsive action or reactive torque. The inertial matter (MR) impacted per second expresses the action function $MR^2\Omega$ rather than momentum $MR\Omega$, with decreasing orthogonality of impulses on shorter radii. To obtain the reverse torque, Equation (5) must be integrated.

$$T_b = \int (\rho^{2/3} C cos\theta R^2\Omega/\sec)dR = \int (MR^2\Omega/\sec)dR\ [\mathrm{ML^2T^{-2}}, \mathrm{Nm}](\mathrm{kg.m^2\ per\ sec^2}) \quad (5)$$

The surface area swept aside by the blade for each 1 m segment of the length L is $C\cos\theta$, given that the radius is varied to estimate torque for each decrease in the length of the blade. So the momentum generated in each second at each radius is equal to the volume swept aside per second ($C\cos\theta R\Omega$ × density ρ/s = $MR\Omega$/s), expressed as an action impulse depending on the radius that gives action per second or torque [$\rho C\cos\theta R^2\Omega$/s] or [$MR^2\Omega$/s, $\mathrm{ML^2T^{-2}}$]. The longer the radius, the more orthogonal the impulse and the effectiveness of the action impact [mrv, J.s]. Equation (5) when integrated with respect to radius suggests that the back torque, while holding the tip speed ratio to wind speed constant, is proportional to the cube of the radius ($T_b = \rho^{2/3} C\cos\theta\Omega L^3/3$).

Subtracted from the windward torque exerted on the front of the rotor blade to obtain the net torque on the rotor, then multiplied by the number of blades and by the angular frequency Ω, the net power P can be obtained. Both torque equations can be derived with a constant value for any configuration of rotor operation and then integrated in a standard formula for R and R^2, respectively [integrals of $L^2/2$ and $L^3/3$] for accurate outputs, assuming ideal conditions. Taking the derivative of factors such as angle of incidence, tip speed ratio (λ), and rotor length (L) with respect to power allows optimization of each of these factors. This should allow ease of control of these factors in wind turbine operation. Optimum tip speed ratios are usually in the range of 3–10 with optimum length a function of wind speed.

Then turbine power (P) generated from wind can be estimated by the difference of windward and leeward torques multiplied by the angular frequency (Ω) of rotation (Equation (6)). Obviously, inefficiencies of the drive train, generator, and power electronics will act to diminish this ideal estimate. These losses in power are not considered in this article, although they should be minimized.

$$P = (T_w - T_b)\Omega \quad [\mathrm{ML^2T^3J}/\sec] \quad (6)$$

Consistent with this introduction, a computer program described in Supplementary Text was used to develop the theory, giving results consistent with Equations (4)–(6).

2.4. Computation

The numerical computer programs given in Supplementary Materials available online employed inputs including wind speed (v), angle of wind incidence (θ), and tip speed relative to wind

Table 1
Commercial wind turbines used for testing the radial action model

Turbine model	Claim	Blade length (m)	Chord width (m)	Blade area (m^2)
Vevor 400	0.400 kW	0.520 + 0.10 hub	0.023–0.115	0.105
GE 1.5MW	1.50 MW	38.75	0.10–3.025	183.0
Nordex N60	1.35 MW	30 + 1.0	0.25–3.25	120.0
Nordex N131	3.90 MW	63 + 2.5	0.25–5.0	487.5
GE Haliade-X	13 MW	100 + 8.5 stalk	0.5–8.00	1290.0

Chord widths as commercial-in-confidence were estimated from advertising material

speed (λ), defining a managed angular velocity [Ω, radians s^{-1}] for the turbines. The complexity of current BEM models suggested that a simpler means to determine wind power based on causative physical principles was needed. Equations (4) and (5) were determined as results by careful attention to physical dimensions (ML^2/T^2), confirmed by the variations in the torques observed in the numerical model, as predicted by theory. A key specification was that the radial action wind turbine model should give good results for wide variations in the power outputs predicted, varying with rotor length and blade area from watts to megawatts.

To test the new theory, estimates were made using dimensions from commercial wind turbines, assuming chord widths as shown in Table 1.

Figure 3 gives a flow sheet and pseudo-coding in program Turbine/Cal for estimation of windward (T_w) and leeward (T_b) torques and maximum power. Programs estimate anticyclone wind speed and energy in the vortical power of wind (Kennedy & Hodzic, 2023) in locations 0823-2506 and then numerical solutions for torques in locations 2507-3563, given turbine parameters including shape, surface area, and pitch to the plane of blade rotation and wind speeds are given in Supplementary Materials. The use of the convenient decrement non-zero (dec JPNZ) instruction enables blade length to be entered into memory (m00) and then decremented numerically to zero repeating the code for label *T*, thus applying the formula to calculate action rate or torque to each element of the blade. Normally, torque is calculated from the product of Newtonian force by length ($m\omega^2 \times r = mr^2\omega^2$). However, a consistent approach in action mechanics is to consider the product of action ($mr^2\omega d\theta$) and its rate of variation ($mr^2\omega d\theta/dt = mr^2\omega^2$).

3. Results

3.1. Power estimates for simulated commercial wind turbines

To test the radial action-torque theory, the selection of commercial turbines given in Table 1 was used for estimating maximum power output from vortical energy by Equation (6). Using available data on blade lengths and estimated chords a set of power outputs, assuming a triangular blade without twist with an angle of wind incidence (θ) 55° and tip speed ratio (λ), the

Figure 3
Computing flow sheet and pseudo coding. Request Supplementary Materials for full details of programs and data. Code locations in Turbine5/cal are shown

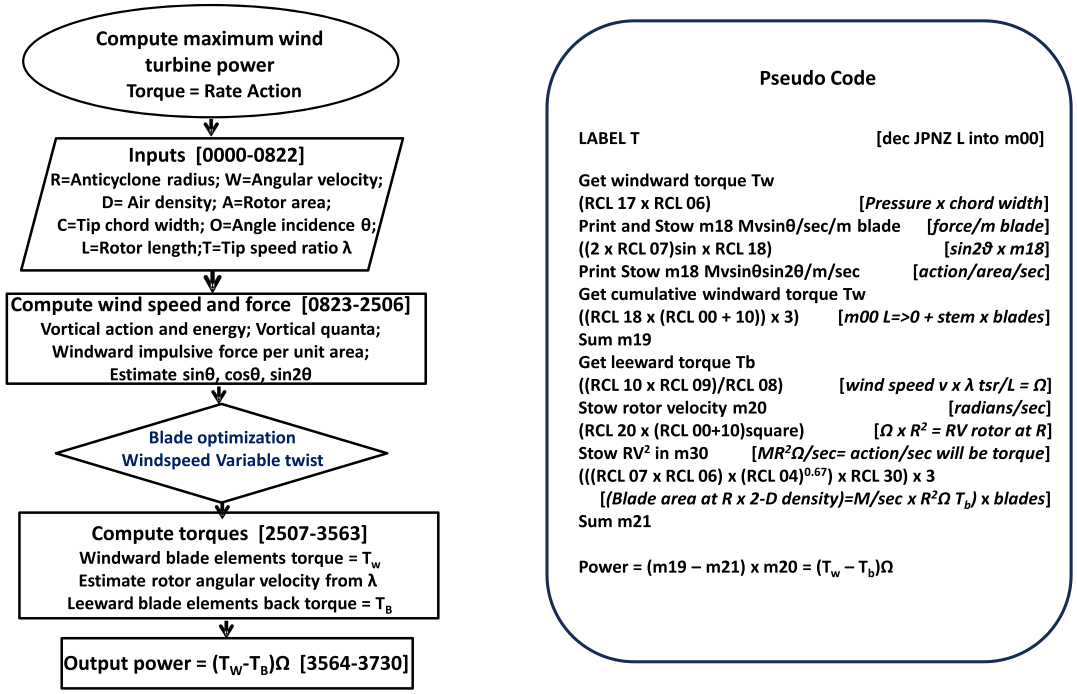

Table 2
Power outputs from simulated commercial wind turbines

Brand	TSR (λ) $L\Omega/V_w$	Wind m/s	Chord C meters	Wind torque (Tw) MNm	Reverse torque (Tb) MNm	Advertised power	Estimated power
Vevor 400	3	15	0.112	0.0000071229	0.00000006913	0.60 kW	0.6104 kW
Nordex N60	8	15	3.250	0.41318	0.07557 (5.6%)	1.35 MW	1.350 MW
GE 1.5MW	8	15	3.025	0.61191	0.11339 (7.0%)	1.50 MW	1.5438 MW
Nordex N131	9	15	3.500	3.46481	0.76443 (16.7%)	3.90 MW	4.5572 MW
GE Haliade-X	10	15	8.000	11.41320	2.72240 (20.8%)	12–14.0 MW	13.036 MW

results are given in Table 2. No attempt has been made in these estimates to optimize aerodynamics, with the windward and leeward surfaces considered as flat and fully elastic. However, it is anticipated that attention to the aerodynamics would produce some marginal effects on power output. Despite a 200-fold range in blade lengths, a close relationship was found between commercially claimed power outputs and estimates from Equation (6).

Only in the case of the Vevor and Nordex N60 was performance data available to the authors, with 0.400 kW at 12 m/s wind speed and 1.13 MW at 15 m/s being claimed. Of several large turbines examined, Nordex claims were found to be the most modest, with claims of 1.3 and 3.9 MW available in advertising material; several of the larger turbines about to be commissioned for marine settings may be too optimistic because of back torque, particularly when the rating was conducted with wind speed close to 10 m/s. Some successful field trials over 24 h may have been conducted with wind speeds sometimes greater than the rating speed. Our radial action model predicts that the reverse torque that diminishes power is a function of blade length, shown in Table 2 as percentage of net power except for the Vevor 400 where it is negligible. This effect of the blade length is a testable prediction of which turbine engineers may already be aware.

Wind angle of blade incidence is $\theta = 55^{o}$; tip speed ratios (λ) were estimated from blade lengths advertised by manufacturers.

A requirement for the radial action model for turbines was that it should be fully scalable with size. Figure 4 shows power results calculated for a wind turbine fitted with 52 cm blades, equal to those of the Vevor commercial model we purchased. Vevor claim power output of the order shown in advertising literature. These results were obtained for triangular blades of average chord width of 6.50 cm, tapering from 2.30 cm at the tip 62.0 cm from the hub to 11.50 cm at the base, supported on a 10 cm stalk to the hub.

Unlike the larger GE 1.5MW and Haliade-X 12MW turbines, the back torque (T_b) was negligible (Table 1), reflecting the shorter radius and the R^2 factor involved. For the Vevor turbine, the theoretical tip speed ratio (λ) shown in Figure 4 above 4 is excessive, exceeding the limit of 800 rpm by the manufacturer's guarantee. The program advanced chord width by 0.1769 cm for each iteration. When data for the Vevor turbine were employed for a rating wind speed of 12 m/s with λ of 3.5, a power output of 406 Watts was calculated. This result is in good agreement with the published rating of 400 Watts. This result is consistent with an accuracy of the radial action model, but it should be experimentally tested in the field.

3.2. Estimates of predicted power output varying wind speed and tip speed ratio

Some representative results included in Supplementary Text using the radial action model varying wind speed and tip speed ratio similar to those expected for a General Electric 1.5 MW wind turbine of 83 m diameter are given in Figure 5. The data show how the windward [T_w] and leeward [T_b] torques differ in character. The former shows a peak close to 55° diminishing toward 0° and 90°. By contrast, the leeward torque is maximal near 0° angle [θ] of incidence, decreasing slowly with the true angle of incidence to zero at 90°. Assuming a constant angular velocity, the potential power output shown in the figure has a similar form to the windward torque. The curves assume a given tip speed ratio λ and rotational velocity. However, where there is no net torque (T_w-T_b) the rotor will not commence or will stall at that angle of incidence. At a wind speed of 10 m/s, the optimum value of λ was 8, but when wind speed is 20 m/s, the optimum ratio was even greater than 20, a value challenging to the strength of materials, since the tip speed would then be 400 m/s, nearing the speed of sound in air.

3.3. Comparing wind's kinetic with vortical energy

From action mechanics we have proposed (Kennedy & Hodzic, 2023; Veers et al., 2019) that air in anticyclones and cyclones, subject to the inertial Coriolis effect, possesses a higher degree of freedom of action superior to the accepted vibrational, rotational, and translational degrees of freedom. This increased reversible sink for energy can be estimated from its vortical action, capable of magnifying the heat capacity of air, depending on the radius of action and the vortical frequency or wind speed ($v = r\omega$). By comparison, the kinetic energy of vortical motion has only a small fraction of the same energy capacity.

This is a testable hypothesis since it predicts that detectable thermal energy will be released as radiant heat from the cascade of turbulent conditions. Furthermore, colliding air masses must also generate radiant heat as laminar flow is replaced by turbulence. We consider it is normal function of anticyclones that they should release radiant heat by friction with the surface (Kennedy & Hodzic, 2023), an important natural process transferring heat from the Hadley circulation of tropical air toward the poles. Too much interference with such natural energy flows could lead to intrusion of colder polar air; this may already be occurring in the polar vortices being experienced in both hemispheres.

We had originally assumed from our analysis of the Gibbs quantum field in the Carnot cycle that vortical energy filling a higher degree of freedom of vortical action in anticyclones and cyclones could be obtained using ambient temperature T expressed as Kelvin. For 3-dimensional translation of molecules like argon or nitrogen mv^2 is equal to $3kT$. For a 3-dimensional velocity v, the temperature (T) must equal $mv^2/3k$, where the translational velocity (v) is 3-dimensional for each gas molecule. By contrast taking a 1-dimensional velocity ($v = r\omega$) as in horizontal wind in an anticyclone, we conclude the equivalent temperature (τ) must equal mv^2/k where v is the wind speed. With

Figure 4
Radial action power output in milli-watts estimated for the Vevor 52 cm turbine showing (a) optima for 55–60° wind incidence θ and (b) increasing power with tip speed ratio λ at all wind speeds. Data for torques *T*w and *T*b are given in Tables S1 and S2 in Supplementary Materials

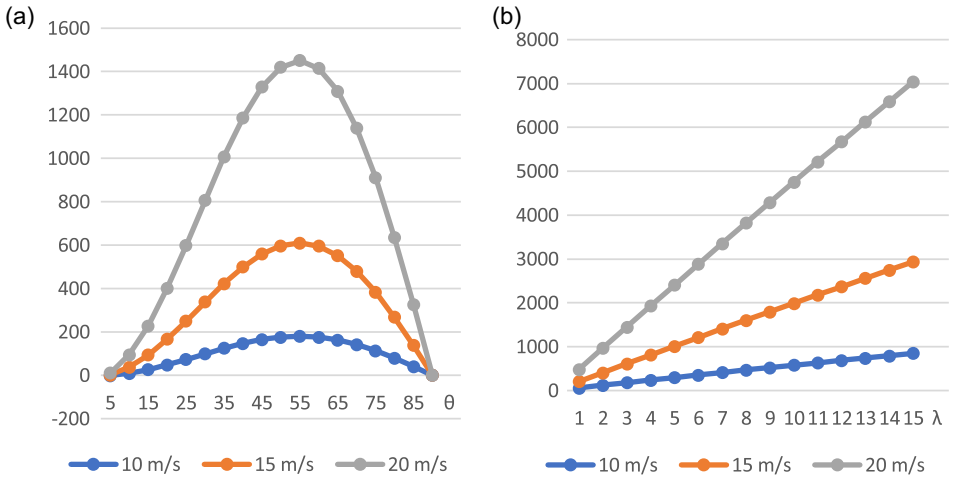

Figure 5
Power simulation of 1.5MW turbine using the Wind turbine Python program in Table S8. A tip speed ratio of 8 was used for four wind speeds of 5, 10, 15, and 20 m/s used for the power diagrams, varying the angle of wind incidence θ (lower panel). Data for varying tip speed ratios are given in Supplementary Materials Table S3

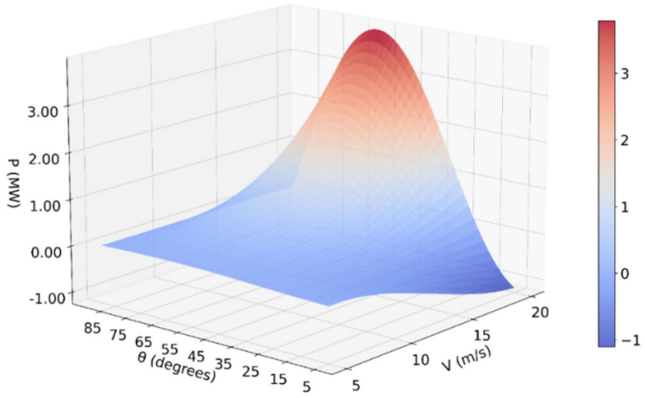

the assumption that temperature is a statistical version of torque as given in our action revision of the Carnot cycle (Kennedy & Hodzic, 2021; Kennedy & Hodzic, 2023), the calculation of mean value negative Gibbs energy must involve the following formula, replacing ambient temperature T for air molecules with τ specific to the Gibbs quantum field (Kennedy & Hodzic, 2023) of wind velocity. Then for an air molecule with wind velocity of v, the virtual wind temperature (τ) must equal mv^2/k.

$$-g_{vor} = mv^2\ln(n_{vor}) = s_{vor}\tau \quad (7)$$

Table 2 provides details of data for vortical energy for a cubic meter of air as wind 1000 km from the center of an anticyclone. The greater magnitude of the vortical component indicates that wind power is not so primary function of kinetic energy but more of the vortical energy of the Gibbs quantum field exerting torques (Kennedy & Hodzic, 2023), supporting the motion of the molecules. Calculation of vortical action ($@_{vor}$) and energy is shown in Equation (8), where r is the radial distance to the center of the cyclonic structure and $r\omega$ is the steady wind speed at R from the center.

$$@_{vor} = mr^2\omega; mr^2\omega/\hbar = n_{vor}; \text{Vortical energy per molecule} = mv^2\ln[n_{vor}] \quad (8)$$

The relative vortical action and quantum state (n_{vor}) are proportional to wind speed, but the vortical energy and quantum field pressure (energy/unit volume) are logarithmic functions of the action as quantum numbers. The mean quantum size is exceedingly small and decreases with wind speed, most of the work or quantum pressure driving the motion of anticyclones (or cyclones) being acquired at lower temperature and wind speed. Given that air at 288.15 K and 1 atm pressure contains 2.5294×10^{25} molecules of air per cubic meter, the vortical field energy of air is 10.052 kJ per cubic meter at a wind speed of 15 m/s (Table 2). For this calculation, we assumed a mean mass of 29 Daltons for air molecules to estimate action.

For comparison, Table 3 gives results for associated wind kinetic energy with various wind speeds, showing data corrected for the Betz limit of 0.593 for the maximum power said to be extractable. Compared to the rate of kinetic energy of wind passing into the total area swept by the blades, the radial action prediction of power is always less, so if a mechanism to harvest the kinetic energy was available, this would be sufficient. However, when the kinetic energy in the wind actually impacting on the blade area is estimated, this is insufficient to explain the predicted power output of 1.5MW. By contrast, when the vortical energy is estimated (Kennedy et al., 2021) acting on the blades is compared, this is greater than the kinetic energy and exceeds the actual power output estimated by about six times, almost an order of magnitude greater. Given the area for three blades is only about 4% of the total swept area, most of the vortical energy in air downwind after wind turbine power is extracted.

Table 3
Vortical energy properties for GE 1.5 MW wind turbine

Wind speed (m s^{-1})	Vortical action ($@_v$)/molecule [J.s, × 10^{19}]	Quantum number n_{vor} × 10^{-15}	1-D torque mv^2/molecule × 10^{24}	Vortical energy /molecule [$(mv^2)\ln(n_{vor})$, × 10^{23} J]	Vortical energy [J/m^3]	Kinetic energy [J/m^3]	Ratio
5.0	2.4215	2.29615	1.2108	4.2826	1083.251	15.313	70.741
10.0	4.8430	4.59230	4.8430	17.4654	4417.740	61.250	72.126
15.0	7.2645	6.88845	10.8968	39.7391	10051.703	137.813	72.937
20.0	9.6860	9.18975	19.372	71.2054	18010.864	245.000	73.514

Radius = 1000 km; action is a function of radius as well as wind speed, shown in Equation (8)

It is predicted that some of the even larger turbines planned for ocean platforms may not achieve the performance anticipated. Given that the back torque is a function of the third power of the blade length when integrated, whereas the windward torque is a function of the blade length squared, a decrease in performance with increasing blade length is expected. These values were all calculated with chord length diminishing from the hub to a small fraction of the maximum width, reducing this negative effect. The estimates in Table 3 are not claimed to be accurate. Chord widths are confidential and have been estimated from photographs. No account has been taken of the rate of twisting of the blades. Such reduction in the pitch near the tip selectively reduces the back torque.

3.4. Relating vortical energy and Gibbs quantum fields with the governing equation of fluid motion

The governing equations of fluid motion as formulated by Bernoulli, Laplace, and others (Kennedy & Hodzic, 2023) proposed no such reversible heat-work process for vortices, except absorption and release of heat depending on whether air is expanding or being compressed as in adiabatic processes. For streamlines as in a laminar wind flow, the Bernoulli Equation (9) relates kinetic energy ($\rho v^2/2$), the static pressure energy P ($\Sigma mv^2/3 = pV$), and gravitational potential energy, regarded overall in steady flow as constant.

$$\rho v^2/2 + P + \rho gh = K \tag{9}$$

The equation is also the basis of the theory that the pressure on the longer profile of an airfoil will be lower, given that $\rho v^2/2 + P$ should be constant. The greater velocity required for air flow with a longer path requires that the pressure P must fall, reducing the downward force. Despite widespread acceptance of this theory, clear evidence for confirmation is difficult to find.

The vortical energy first proposed in Kennedy and Hodzic (2021) as $S_{vort}T$ but now revised must be added to the total heat content indicated by the Clausius entropy of air, with the vortical component able to be released in compressive or turbulent frictional processes. The same categories of energy transformation are also observed in the Carnot cycle, varying during the isothermal and adiabatic stages. We have extended this hypothesis (Kennedy & Hodzic, 2023) to show how this internal work that Clausius named the ergal amounts to a decrease in the Gibbs energy in Equation (10). To the extent that the vortical motion provides an additional degree of freedom for energy storage at a larger scale, another term needs to be added to the Bernoulli equation.

$$\rho v^2/2 + P + \rho gh + S_{vort}T = K + Nk\tau ln(@_{vort}/\hbar) \tag{10}$$

Here, the Kelvin scale for temperature and S_{vort} are not considered as appropriate given that the corresponding magnitude of torque exerted is required, effectively a much lower temperature as τ. This can be thought of as a radial form of quantum state or potential energy, capable of being released in defined meteorological conditions. We refer to this resonant energy as the Gibbs quantum field (-G) and it comprises an addition to Clausius' ergal as a work process internal to the atmosphere (Kennedy & Hodzic, 2023).

3.5. Evidence of vortical heat produced by wind farms

In a previous paper, Kennedy and Hodzic (2021) showed that surface air heated from absolute zero to 298.15 K needs 2.4 MJ of thermal energy per cubic meter, including its kinetic energy. This implies that the vortical energy of air in laminar flow at 1000 km of 15 m/s from the center of an active anticyclone contains about 0.42% more wind-reversible field energy than at its non-rotating center. The data in Tables 3 and 4 of possible heat capacities in the wind suggest an alternative explanation. This source would be the release of latent heat in wind of vortical energy, a result of turbulence caused by turbines. The concept of vortical entropy was advanced by a new class of potential risk to be considered in climate change. The kinetic energy of wind of 10 m/s is only 61 J per cubic meter.

Should the laminar flow be impeded by surface roughness, causing turbulence, some of the vortical energy will be released, warming the surroundings. For example, as detailed in Table 4, if wind speed of 20 m/s is effectively reduced by turbulence to a speed of 10 m/s, some 54 MW of vortical turbulent heat is predicted to be released from air impacting the blades, heating the surrounding molecules moving downwind. Given a heat capacity of 1.225 kJ per cubic meter for air, this is sufficient to heat 6122 m^3 of air 1°C. A wind farm 1 km wide generating 100 MW of power from 70 GE 1.5MW turbines is predicted to release 3800 MW of heat, moving 3.1 million m^3 of air 10 m downwind a second, raising air temperature 3°C in a column about 100 m high. This prediction can readily be directly tested, possibly consistent with published observations of warming by wind farms, given downwind turbulent heat must be dispersed.

Table 4
Kinetic and vortical energy impacting a wind turbine similar to GE 1.5MW

Wind speed (m/s)	Kinetic energy per second 83 m diam. (Betz) (J)	Kinetic energy / blade-area/s blades	Vortical pressure (J/m^3) (blade area x *v*)	Vortical power (Watts, J/s) estimated for blade area	Power estimated by radial action model (Watts)
					At $\lambda = 9$, $\theta = 55^o$
5.0	2.1670×10^5	8.4066×10^3	0.361069×10^3	0.33038×10^6	0.031168×10^6
10.0	1.7336×10^6	6.7253×10^4	1.47258×10^3	2.69482×10^6	0.40541×10^6
15.0	5.8509×10^6	2.2698×10^5	3.35055×10^3	9.19727×10^6	1.54381×10^6
20.0	1.3869×10^7	5.3802×10^5	6.00353×10^3	21.9729×10^6	3.86798×10^6

3.6. Environmental effects of heat production

Given the prediction of significant heat production in Section 3.5, the environmental effects of wind farms should be of concern. In particular, their potential effect on evapotranspiration downwind as a result of turbulence should be considered. Application of the Penman–Monteith equation is the usual method to model evapotranspiration, including evaporation from soil or water surfaces as well as transpiration of water used by plants to absorb nutrients, maintain plant turgor, and provide water for photosynthesis. Despite its importance for plant growth in the assimilation of carbon dioxide, the actual consumption of water for plant growth is far less than that transpired. The inputs required are daily mean temperature, wind speed, relative humidity, and solar radiation. To assist investigation of causes and effects for these events affecting bushfire risk, we are employing the Penman–Monteith equation (Allen, 2005), with data potentially of use from the MODIS satellite.

In Equation (11) for evapotranspiration (*ET*), factors *R*n and *G* indicate solar radiation and local absorption of heat into the soil, ρ_a represents atmospheric density, C_p the heat capacity of air, e_s^o mean saturated vapour pressure (kPa), r_{av} bulk surface aerodynamic resistance for water vapor, e_s mean daily ambient vapor pressure (kPa), and r_s the canopy surface resistance (s m^{-1}).

$$ET_{sz} = \frac{[\Delta(Rn - G)] + \left[86,400 \frac{\rho_a C_p}{r_{av}} (e_s^o - e^a)\right]}{(\Delta + \gamma\left(1 + \frac{r_s}{r_{av}}\right)} \qquad (11)$$

Wind speed *u* is also included in the numerator. The main drivers of evapotranspiration are heat from solar radiation, plant growth, environmental conditions of temperature, and relative humidity as well as transport away in air. More important than wind speed, turbulence has now been shown to significantly increase evaporation, as eddy diffusion lengthens the trajectory for water vapor molecules. Since terrestrial wind farms are usually placed in rural areas, we are applying this model to test our prediction that they may contribute to dehydration of the landscape downwind from turbines, increasing fire risk. We will discuss how these proposals may be tested experimentally, including by observations from the MODIS satellite.

To determine the potential effects of wind turbines on evapotranspiration, we calculated evapotranspiration at a range of wind speeds and then recalculated it with 1 and 3°C increases in temperature assumed to be the result of wind turbines (Table 5). A 1 degree increase in temperature was used as we found from that turbulence caused in the wind at 20 m/s by wind turbine blades effectively reducing laminar speed to 10 m/s which could release enough heat to raise the temperature downwind in a swath of 100 m wide and 250 m high more than 50 km downwind by 1°C. We used the Penman–Monteith equation for the 5th February at -30.39 latitude, 275 m elevation, and assumed effective daylength of 9.25 h.

The FAO version of the Penman–Monteith equation was applied using the python module ETo, and only the values described here were altered. For both temperature and relative humidity, minimum and maximum values were 20 and 30°C, and 25% and 84%. Evapotranspiration rates calculated without heat input from turbulence induced by the wind turbines are compared with rates corrected with a 1 degree increase in minimum and maximum temperatures, with all else unchanged. The evapotranspiration is between 0.21 mm/day at 5 m/s to 0.58 mm/day at 25 m/s. These predictions, and the short- and long-term effects on the dryness of soil and plants, need to be tested experimentally. Clearly, at elevated wind speeds over multiple consecutive warm to hot days, the additional quantity of moisture removed from the soil and vegetation due to wind turbines has the potential to be substantial. Our calculation in Table 6 has taken no account of the downwind turbulence that may increase evapotranspiration significantly (Cleugh, 1998; Navaz et al., 2008).

If these predicted results are confirmed experimentally in rural landscapes where wind farms are located, they would indicate increased risk with respect to optimum agricultural or pastoral productivity. However, in some cases increased temperature and reduced water-holding capacity of air may be beneficial for plant growth, particularly in environments with ample water supplies. By contrast, in drought prone conditions like most of Australia, negative effects on productivity and increased fire risk can be assumed. There is a need for these factors to be assessed wherever wind farms are developed. Recently, attention was drawn (Wang et al., 2023) to the observation that soils in areas with wind farms in Germany have lower moisture contents than in other areas. This is predicted by the analysis in Section 3.6. Furthermore, other studies have shown how downwind turbulence wakes may extend many kilometers from the perimeters of wind farms (Barthelmie & Pryor, 2019; Nygaard, 2014; Platis et al., 2018), consistent with such downstream drying of soils.

4. Discussion

The radial action model for wind turbines emerged from doubts regarding sufficient kinematic potential in an imaginative search for alternative hypotheses that could be tested, science as recommended by the late Karl Popper. The initial computer program described in Methods section was developed by a reiterative process. Equations (4) and (5) became available only after this process was complete when results and experience with real wind turbines were found in agreement. It is doubtful if this result could have been achieved with a higher-level computer language. Equations (4) and (5) can be used in modeling with other computer codes, like Python and Mathematica given in Supplementary Materials.

Table 5
Potential for heat release from turbulence caused by 1.5 MW wind turbines

Turbulent process	Vortical energy J/m^3	Heat released J/turbine/s	Heat released wind farm 70 GE units J/s	Volume air heated 3°C, m^3/s	Height of warmer air moved 10 m/s
Difference 20 declined to 10 m/s	13593.26	5.4370×10^7 200 m^2 blades, 20 m/s	3.8059×10^9	1.036×10^6 C_p 1.225×10^3/m^3	103.6 m 1 km wide front

The calculations of wind power to the cube of wind speed shown in Equations (1) and (2) consider the rate at which kinetic energy of air flows through the circular profile area traced by the tips of the rotors. However, only a fraction of this air can be intercepted by the blades, despite appeal to concepts like solidity with respect to the air flow. Particularly in the larger modern turbines most of the air flow passes through unimpeded, given that the blades normally represent only some 3–4% of the area of the rotor circle. Thus, it is likely that no more than 5% of the air volume is initially made turbulent, effectively tracing triplicate rotary spirals of turbulent air downwind, balancing the work done on the turbine rotors for transmission into the dynamo.

The leeward torque absent from BEM theory performs work normal to the air flowing into the cavity behind the blade, up to about 21% of the power generated (Table 1) at 100 m blade length. Additional release of radiant heat by turbulence is predicted to be a feature of the operation of wind turbines, possibly more than five times power generation if the vortical energy hypothesis is confirmed. We hypothesize a significant warming effect downwind that may also increase evaporation, caused by temperature increase and turbulent surface interaction with vegetation and soil surfaces. This prediction should be tested for quantification, to be included in productivity models or estimates of fire risk, as a matter of due diligence.

4.1. Reconciliation of radial action and BEM models

The theoretical success of this model calls for some comparison with the BEM model based on airfoil and Bernoulli fluid motion partial differential equations (Batchelor, 1967). In Figure 2, aspects of the two different approaches were given on one diagram. Only a small proportion of the air stream will impact the blades depending on the proportional area of the circle with radius *L*.

If stationary, obstruction by the blade must create a region of low pressure to its rear. Once a steady state of rotation Ω is reached, the blade still obstructs air flow as before but its rear surface impacts resisting air normal to the blade's motion, deflecting it with the action impulses a function of the radial speed of rotation ($R\Omega$). For most of the blade except near the hub, the pressure at the rear of the rotating blade must be increased above that in the wind. However, there is no diminution of pressure exerted on the windward surface because fresh air continually occupies this space. Except near the hub, air at the rear of the blade is strongly compressed so that no drag in the same direction as the wind is possible, turbulence caused by diminished pressure. The windward impact pressure is independent of the radius unless the blade is pitched with length, varying by sin θ, affecting the volume of air impacting the blades per second. While the intensity of impulses is constant for a blade surface with a constant pitch, the rate of action or torque varies with radius, requiring integration for the turbine. By contrast, the impulses produced by the leeward surface of the blades vary with the radius squared, once for the air impacted normal to the rotation per second and once more for the radial variation in momentum as action impulses.

There is no intention to repeat a description of BEM theory, performed in detail by Schubel and Crossley (2012). However, in using their Bernoulli approach to airfoil theory BEM considers lift normal to the blade and drag directed horizontally along the surface in the wind direction as the two main forces operating. To determine relative wind velocity the variable speed of an observation point on the rotating blade is taken. If near the hub, there is little change of direction (θ–β) but near the tip, the apparent angle of incidence diminishes. Alternatively, the pitch may be increased to 90°, when the back torque, while the blade is still spinning, will exceed the almost zero windward torque. Many of the performance studies on horizontal turbines have been performed with "frozen" rotors (Zhu et al., 2014), experiments conducted with variable speeds in wind tunnels enabling theoretical power to be calculated. However, BEM avoids consideration of back torque that impedes rotation.

We emphasize that the main purpose of this article is to develop a testable hypothesis explaining the maximum power in an ideal wind turbine, assuming the output is linked reversibly to a work process such as electricity generation. This purpose is similar to

Table 6
Predictions regarding heat production and evapotranspiration for 1 and 3°C change in minimum and maximum temperature on wind farms

Wind speed (m/s)	Evapotranspiration	Evapotranspiration	Delta ET (mm/day)
Heat increase 1°C	No wind farm	With wind farm	
5.0	6.20	6.39	0.19
10.0	8.44	8.74	0.30
15.0	9.83	10.21	0.38
20.0	10.78	11.23	0.45
25.0	11.47	11.96	0.49
Heat increase 3°C			
5.0	6.20	6.77	0.57
10.0	8.44	9.35	0.91
15.0	9.83	11.01	1.18
20.0	10.78	12.16	1.38
25.0	11.47	13.00	1.53

Figure 6

Common Newtonian lift forces for air foils and wind turbine blades. For both cases, the action of deflection of wind momentum is conserved, requiring that the component of cross momentum normal to the initial wind direction acts as a reaction rotating the blade or the foil. Since the air foils are balanced on the aircraft and rotation is normally prevented, the lifting forces proportional to sin2θ in effect render the aircraft weightless in level flight

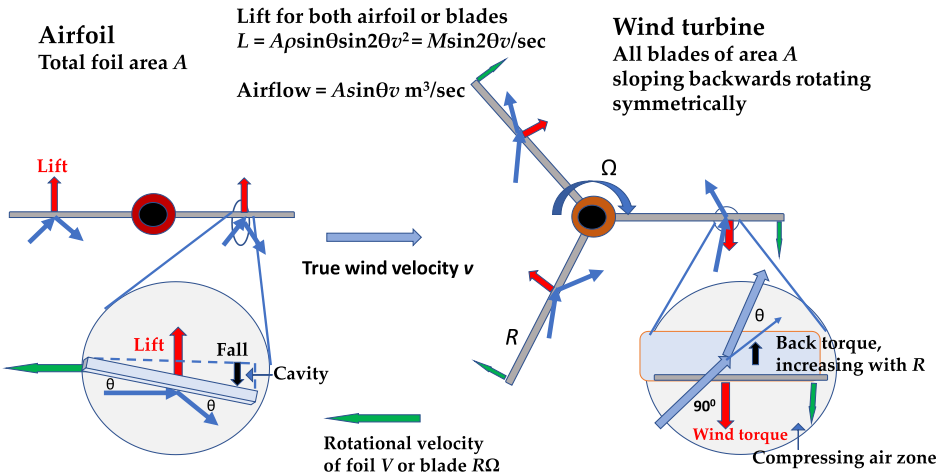

Sadi Carnot's proposal that the main purpose of his heat engine cycle was to describe the most efficient cycle. However, the environmental effect of turbulence must be examined as it is a key consequence of the radial action hypothesis because of the greater magnitude of energy available subject to possible dissipation.

4.2. A surprising equivalence of turbine theory to that for lift in Boeing 747 air foils

Comparing impulsive action mechanics with actuator disc BEM, if two mathematical models give similar results this implies that both operate from similar causes, even if expressed in different formulae. While BEM uses an air foil approach, action mechanics uses momentum as its conservative principle. This requires that the angular deflection of $Mv\sin2\theta$ in the wind momentum with respect to the wind direction caused by the blade must be compensated by an equal reaction component of reverse momentum available to power turbine blade rotation. Since the volume of air per second impacting the blade is proportional to $\sin\theta$, the rate of deflection of momentum is equal to $A\rho\sin\theta\sin2\theta v^2$ per second inserting terms for area (A), density of air (ρ), and wind velocity (v). As with the wind turbine, the square of the velocity is needed to establish the volume of air impacting underneath the foil per second, as well as the rate of momentum impacting the foil. This formula is the basis of Equation (1) developed earlier, here exerting a lift force normal to the wind.

While revising this article for resubmission, the question arose whether the same momentum equation used for turbines might also be applicable to air foils. This follows the demonstration in Figure 2 that the idea of drag for non-rotating air foils could be inappropriate for a turbine rotor, at least at blade radii where rotor velocity exceeds wind speed so that momentum was transferred from the blade to air at the rear of the blade. If surface drag over the blade was not operative on turbine blades except close to the hub, could the effect of drag in air flow over foils also be inappropriate, although the whole aircraft would cause drag as resistance to forward motion? A tendency to lower pressure above the foil is logically a result of continuous air depletion, equal to the volume of air deflected underneath the foil. In accord with a process of least or most rapid action, this void or cavity must be filled continuously with air accelerated from directly above the foil, part of the air column close to 10,000 kg mass (M) of air molecules per square meter, a weight of 9.807M. Depending on the angle of attack of the foil, this air would then fall a maximum height of $C\sin\theta$ continuously into this cavity reaching a velocity of $(gC\sin\theta)^{0.5}$ m/s on the rear edge of the foil (Figure 6). This rate of falling momentum or impulse on the foil establishes an impulsive force directly opposed to the lift from the rate of momentum deflected downwards.

In Table 7, the action mechanics method for lift is applied to the flight of a Boeing 747 804, estimating the pitch or angle of attack required for a forward speed of 80 m/s needed to counter the mass of the loaded aircraft of 398 tonnes. The fall column estimates the rate of the impact of the weight of the falling air column into the cavity for different angles of attack. This suggests that takeoff is achievable for an engine thrust achieving a forward speed of 80 m/s at about 14º, where net lift is sufficiently positive to gain elevation.

If the pitch or angle of attack is increased without increased thrust and thus of the airflow, the resistance or drag must increase, causing stall because of inadequate airflow to provide the lift required. It is assumed in Table 7 that forward speed is maintained, requiring more thrust. The stall pitch is estimated by air foil theory as about 15°, just over the 13° for conditions in Table 7 appearing to produce a net lift sufficient for the Boeing 747 aircraft to take off at a runway speed of 288 km per h. In fact, this is typical for the Boeing 747, supporting the action mechanics model.

There is a separate influence of drag or resistance because of turbulence from displacement of air by the aircraft's forward motion, soon restored behind it, but the work needed to counter drag is included in the thrust of the jet engines achieving a forward speed of 80 m/s. This drag will not significantly affect the ability of the air foil to achieve lifting force.

Table 7
Applying radial action and reaction lift to 525 m² air foils of a 397,727 kg Boeing 747, air speed 80 m/s (V)

Pitch angle deg.	Lift (kg/s) $A\sin\theta\rho\sin2\theta v^2 = Mv\sin2\theta/s$	Cavity impact (kg/s) AMg	Cavity fall at rear edge (h m) $C\sin\theta$	Velocity of fall V (m/s)	Foil lift (kg)	Net lift (kg)
5	62,293	33,952	0.669	3.622	28,314	-369,386
10	244,454	47,376	1.333	5.113	197,078	-200,649
15	532,650	56,730	1.986	6.242	478,920	+ 78,192
20	904,887	63,443	2.625	7.175	849,444	+ 443,717

Although the mechanism of flight caused by air foils has often seemed mysterious, this solution shows that the action momentum of deflected air is sufficient to power air flight.

4.3. Wind turbine blade design, twist, and other modulations in rotors

The BEM theory justifies the twisting of the blade, increasing the pitch toward the hub from around 0° approaching the tip (Sørensen, 2016; Schubel & Crossley, 2012). A twist from the optimum angle of incidence (θ) from about 60° near the hub might be justified by diminishing the back torque proportional to R^2 and sinθ nearer the tip. This property can be introduced into the radial action model by increasing the pitch angle from a low value at the tip toward the hub. This is recommended from BEM theory (Schubel & Crossley, 2012) and increases up to 30° have been recommended. This would bring hub values of angles of incidence similar to the optimum of 60°. However, in radial action theory, wind torque (T_w) and back torque (T_b) both diminish to disadvantage with pitch decreasing from the optimum angle to the tip. A low pitch may be justified if high torques exerted near the tip cause excessive turbulence and noise levels. At low wind speeds and low angles of wind incidence, negative values of total torque are found with T_b greater than T_w up to 25°, or pitch of 65°, given the higher value of cosθ controlling back torque. The inability to test large turbines in wind tunnels means that field performance of such variations must be judged empirically, by trial and error. Further airfoil refinements commonly engineered into the rotors can easily be incorporated. These are considered to minimize frictional effects on turbines, making an independent contribution to the efficiency of power output. Incorporating design features that are responsive to wind speed and other factors may optimize this process, confirmed by practical experience.

In Figure 7, the effect of varying angle of incidence for triangular blades also twisted from a pitch of zero at the tip to the chosen final angle of incidence (θ) at three different wind speeds is shown. Figures 4 and 5 and data in earlier tables were estimated using blades with no twist, from hub to tip. The same tip speed ratio is taken throughout, explaining why the angular velocity of the rotor is constant (Ω), except at 90° where it is taken at zero. This figure illustrates how the windward torque Tw is always positive although the back torque can be theoretically calculated as negative if the turbine was turning with the tip speed shown. No power can be generated by wind until the angle of incidence exceeds 25° at 5 m/s, exceeds 15° at 10 m/s, and 10° at 15 m/s. Significantly, more power can theoretically be generated if the same angle of incidence is maintained from the hub to the tip, though the greater back torque near the tip may present

Figure 7
Radial action plots of power output at differing wind speeds and angle of incidence (θ = 1–85°). Program conditions were density 1.225 kg/m³, total blade area 140 m²; blade length, 80 m; tip speed ratio $\lambda = 8$; twist from 0 pitch at tip to θ from 90-θ. δT at 10 m/s is obscured because the angular velocity is 1.0

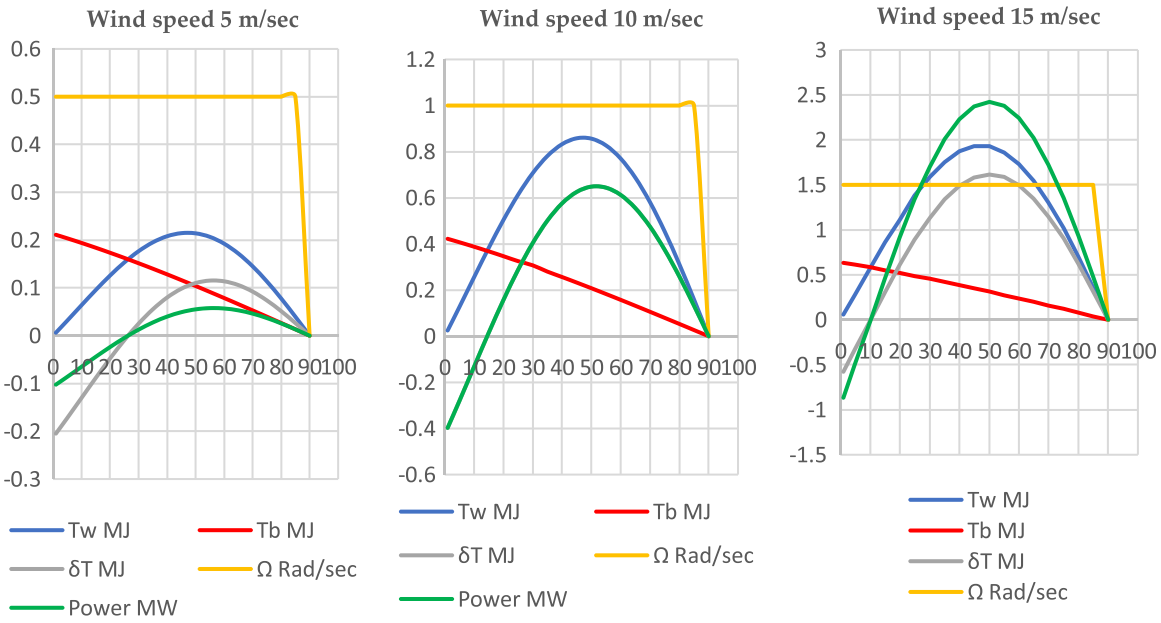

technical problems related to stress of materials or noise. While the back torque declines almost linearly between a pitch of 90° and 0°, the windward torque reaches a maximum for angle of incidence in the range 50–55°. This is consistent with the usual finding that twisting blades from a low pitch near zero at the tip to around 30° is beneficial for power, corresponding to an angle of wind incidence of 60°, nearer to the optimum predicted. Above 40° of twist, radial action predicts power will decline from an angle of incidence of 50°.

The ease of calculation of windward and back torques and power lends the model to application under conditions when sensors can provide feedback on wind speeds and tip speeds allowing changes in pitch angles to suit actual field conditions. The radial action model estimates the maximum power output possible assuming no losses from friction and resulting turbulence for best design. The working computer models can readily include performance factors allowing for losses of efficiency by the various causes, some that are incorporated into BEM as shown in Figure 2.

This new understanding of power generation from radial action theory accepts the value of research on optimizing blade design. Factors such as variation in thickness and twist of the chord pitch will still provide advantages in power output if correctly analyzed by control theory, using Kalman filters for optima. Schubel and Crossley (2012) have provided a detailed review of the current state of the art of blade design, highlighting efficiency to be gained from design principles based on blade shape, airfoil properties, and optimal attack angles using relative wind speed and gravitational and inertial properties (Zhu et al., 2014). With suitable corrections applied, lift and thrust factors and generation of action most of this theory can be remodeled to include inefficiencies.

The Betz limit is considered to exert an effect on BEM theory but has no place in radial action mechanics. Only a small proportion of the available vortical energy is consumed, but a different kind of limit emerges in the competition between windward and leeward torques, with the latter becoming more significant as the length of turbine blades increases.

4.4. Heat production from turbulence

In developing turbulence, the largest scale eddies nearer laminar flow are regarded as containing most of the kinetic energy, whereas smaller eddies are responsible for the viscous dissipation of turbulence kinetic energy. Kolmogorov, as described by Frisch (1995), hypothesized that the intermediate range of length scales could be statistically isotropic, and that a temporary form of equilibrium would depend on the rate at which kinetic energy is dissipated at the smaller scales. Dissipation is regarded as the frictional conversion of mechanical energy to thermal energy, effectively radiation, raising temperature. In vortical action theory, the kinetic energy is regarded as always complemented by quanta of the Gibbs field vortical energy and the dissipation process loses kinetic energy, a result that is coincident with the loss of the supporting field energy. The dissipation rate may be written down in terms of the fluctuating rates of strain in the turbulent flow and the fluid's kinematic viscosity that has dimensions of action per unit mass. We suggest that the failure to obtain analytical solutions for turbulent processes may solved if these complementary forms of energy are considered.

Current practice for wind power makes no provision for heat production other than minimizing friction. The action theory demonstrates that the back torque exerted by turbines is effectively a work-heat dissipation of wind energy, contributing to its evolution locally at the point of power output. Depending on the factors controlling efficiency, this heat production can be considered as less but of the same order as the power take-off as electrical energy. Of more concern could be additional heat release downwind from turbulence. In Table 4, we provided estimates, showing that turbulent release can be significantly greater in magnitude. While direct heat production at the turbine is not expected to make a significant difference to air temperature, together with turbulence, a significant fall in the relative humidity of air passing over vegetation and soil together with greater surface interaction by turbulent air can be anticipated. The vortical degree of freedom of motion or action is characterized by its large radius of action, effectively storing latent heat that can be released as radiation in turbulent conditions. It is known that the kinetic energy in laminar flow is not retained in the turbulent motion of air or water moving on much shorter radii of declining scales. Radial action theory predicts this will be the case, the loss of kinetic energy expected as potential energy we have referred to as Clausius' ergal (Kennedy & Hodzic 2021) as internal work is released. The kinetic motion in the system at all scales is sustained by such quantum state energy. This is a consequence of the virial theorem, also explained by Clausius (Kennedy & Hodzic 2021).

The impacts of wind farms on surface air temperatures are well documented. Baidya Roy and Traiteur (2010) claimed that this regional warming of almost 1°C compared to an adjacent region resulted from enhanced vertical mixing from turbulence generated by wind turbine rotors. Warmer air from above the surface, particularly at night, was claimed to be forced to the surface. Harris et al. (2014) showed night-time warming relative to surrounding areas using observations made from 11 years of MODIS satellite data with pixel size of 1.1 km^2. The same conclusion was reached by Miller and Keith (2018), showing a significant night-time warming effect at 28 operational US wind farms. They also concluded that wind's warming could exceed avoided warming from reduced carbon emissions for more than a century. According to Miller (2020), these effects on warming are detectable tens of kilometers downwind, as are the wakes mentioned earlier (Barthelmie & Pryor, 2019; Nygaard, 2014; Platis et al., 2018), visible from space.

However, the opinion that warming is a result of overturning temperature inverted air at night is not convincing. The observation that warming observed was greater at night is easily explained by stronger laminar flow of air fully charged with vortical energy, significantly dissipated by thermal turbulence in the daytime. The conclusion about overturning is probably based on an argument that this was the only source of warmer air available. The release of only a smaller fraction of vortical heat in turbulent air obviates such reasoning. More direct observations using instruments sensing simultaneously, both upstream and downstream of wind farms, are required to establish the source and extent of warming, particularly in higher daytime temperatures.

4.5. Independent evidence of vortical potential energy as a heat source released by turbulence

Chakirov and Vagapov (2011) describe a method for direct conversion of wind energy into heat using a Joule machine. They show that turbulence in a rotating fluid with Reynolds number (*Re*) greater than 100,000 provides warmth not obtained when the flow remains laminar. By insertion of baffles to cause turbulence in the flow path of water set in rotation in a smooth cylinder

Table 8
Summary of dynamic action mechanisms considered in this article

Action topic	Factors considered	See sections	Significance or consequence
Newton's third law and wind turbines with torques T_w and T_b	Equality of action and reaction and elastic deflection of wind momentum by 2θ from incidence	Figures 1 and 2, Sections 2.1–2.4	A turning moment proportional to the rate of momentum deflected by sin2θ from the angle of incidence (θ) opposed by a back torque
Vortical action and field energy = $mv^2\ln(n_{vor})$	Classical quantum states estimated by quotient of action over Planck's quantum of action	Tables 3 and 4, Section 3.3	Allows calculation of vortical work content in the troposphere and its potential to reverse work as heating from turbulent friction
Turbulent release of vortical energy/heat	Increased curvature of action field, releasing vortical energy	Tables 5 and 6 Section 4.6	Turbulent drying and loss of productivity in downwind landscape
Lift for aircraft foils = Mvsin2θ/s	Deflection of air stream by 2θ and continuous equal evacuation above air foil causing vertical drag	Figure 6, Table 7, Section 4.2	Lift in aircraft proportional Mvsin2θ from the angle of incidence and a partial vacuum above the foil, filled from above

using direct wind power, they demonstrate that needs for room heating in polar regions can be satisfied. It is well known that the kinetic energy in turbulence is not conserved at lower fractal scales, suggesting that any vortical energy or ergal is also lost in these processes, with work performed dissipated as heat by friction. We have recently discussed such heat-work-heat cycles in an action revision of the Carnot cycle, emphasizing the importance of vortical field energy as the negative of the Gibbs energy. The molecular kinetic energy in such systems is a small fraction of the total non-sensible heat, stored in quantum state activations of translation, rotation, and vibration.

Chervenkov et al. (2014) have shown how the kinetic energy and temperature of polar molecules can be reduced with a centrifugal force from around 100 K to 1 K. A redistribution of vortical potential energy from interior molecules that can be retrieved near the center of the centrifuge is regarded as the cause of the cooling. Geyko and Fisch (2013) and Geyko and Fisch (2016) reported measuring reduced compressibility in a spinning gas where thermal energy is stored in their theory of the piezo-thermal effect. This extra heat capacity at constant temperature indicates an additional degree of freedom, that we conclude is vortical, supplementing the well-recognized vibrational, rotational, and translational action as degrees of thermodynamic freedom (Kennedy & Hodzic, 2021).

4.6. The importance of field energy supporting the quantum states for wind power

There is a widespread failure to recognize the dominance of this nonsensible field energy as real potential energy in natural systems. This field was shown to be needed to explain the amount of heat required to heat ideal gases from absolute zero to ambient temperature (Kennedy & Hodzic, 2021), being a multiple of the kinetic energy. Considering only the sensible kinetic energy as indicating the temperature of molecules omits its cause, confirmed when we estimated the entropy of atmospheric gases in our revision of the Carnot cycle (Kennedy & Hodzic, 2021). In effect, potential energy in the atmosphere can be gravitational varying vertically, but much more can be stored horizontally as vortical Gibbs energy. These two forms of energy, kinetic energy and vortical energy as negative Gibbs energy, are complementary in operation and one must always have one to have the other. The viscous dissipation of energy in storms is not just the turbulent kinetic energy released in a turbulent cascade (Businger & Businger, 2001) but also the vortical energy, much larger in magnitude, that sustains the kinetic energy (Kennedy & Hodzic, 2023). In a previous version of this article as a preprint not accepted by Copernicus' Wind Energy Science (Kennedy et al., 2022) our proposal that the Bernoulli equation of continuum mechanics is insufficient to explain wind power was rejected. Neither two reviewers nor three editors were prepared to consider our new proposal seriously. The editor of MDPI's journal Wind also declined this article, despite their invitation to resubmit the first version with only one of five reviewers recommending rejection. We understand that the editors of journals more skilled in theory regarding axial BEM theory consistent with continuum mechanics will be reluctant to admit another paradigm into their journal, although they should be less restrictive reflecting their titles. In our proposal, it is the momentum sustained by the quanta of a Gibbs quantum field that actually does the frictional work (Kennedy & Hodzic, 2021; Kennedy & Hodzic, 2023), causing physical damage in cyclones, a possible fact that should be of interest to all wind scientists.

5. Conclusion

This article was motivated by novel approaches in applying action mechanics, arising from a program of revision based the principle on least or stationary action, first proposed in 2001 (Kennedy & Hodzic, 2021; Kennedy & Hodzic, 2023). This proposal considers efficient causes for physical and biological processes primarily as expressions of least action. As a result, variation in action with time as torque becomes equivalent to force times length, providing an alternative approach for estimating torques on the blades of wind turbines. In this article, this action theory is further developed in Section 2. Furthermore, the recent proposal of vortical action and vortical field energy in anticyclones and cyclones (Kennedy & Hodzic, 2021) as a derivative of action mechanics suggests that winds, particularly in laminar flow, contain far more energy in a potential form storing heat as work of cyclonic motion influenced by the Coriolis acceleration than previously believed. To assist understanding of the consistent physics advanced in this article, a concise summary of the mechanisms proposed that involve impulsive action and its rates of execution as torques is given in Table 8.

Uniquely, by coupling Newtonian or Leibnizian approaches regarding momentum transfer using action mechanics, facilitated by torques as the rate of action impulses from Gibbs quantum fields sustaining winds, we claim to have provided a highly effective method to estimate maximum power extraction from wind turbines. By comparison with the axial BEM model, this new theory can claim the following advantages, subject to experimental refutation or confirmation.

- A more effective mathematical model of wind power output, based quite simply on conservation of deflected momentum. The radial action method allows maximum power to be estimated more directly. We used a similar dynamic approach to revise the Carnot cycle for maximum power of heat engines and for explaining the destructive power of tropical cyclones (Kennedy & Hodzic, 2021).
- A better template for improved wind turbine design is possible, with a more direct correspondence between theory and practice. Key issues to determine will be optimum pitch and blade length as a function of wind speed.
- A possible means for optimization of wind power and to minimize turbulent heat output is now available. This may have the potential to be applied in control theory for managing turbines, either solitary or in wind farms. It is noteworthy that the action mechanics theory developed in this theoretical study suggests that only a minor proportion of the potential power of wind in laminar flow is utilized (Table 3), unlike the BEM theory based on harvesting a significant proportion perhaps up the half of the kinetic energy.
- Surprisingly in an exercise of reverse engineering, very similar mathematical equations as those for radial action in turbines can be applied to the vexed problem (Regis, 2020) of explaining lift in air foils, shown for Boeing aircraft in Table 7; thus, flight depends on the deflection of air stream momentum beneath the wings and countered in part by a continuously replenishing force from the vertical air column into the temporary cavity behind the foil. This finding provides validation for the radial action model for wind turbines.
- We envisage future work with wind turbines by collaboration with field engineers in power companies involved. Prospects include improvement in blade design including varying length with wind speed. Analysis of the downwind air stream using drones for collecting data with appropriate sensors such as degree of turbulence, temperature, and thermal radiation is all of interest. Radial action offers novelty that can be tested appropriately.
- Environmental protection may also be a more easily obtained result using the action model. Ways to manage turbulence to reduce its possible negative effects such as downwind dehydration can be topics for research, seeking to avoid unintended environmental consequences of this burgeoning technology as a prime source of renewable energy.

A feature of wind farms is low power output during periodic wind droughts, particularly in autumn or spring seasons of fine weather in middle latitudes. This may require a 3-fold multiple of plated power capacity to guarantee supply, while large lithium batteries can only help by linking and smoothing of regions, not being capable of significant storage. Australia's widely dispersed eastern grid from South Australia to Queensland, the largest in the world, poses significant security and reliability concerns according to a comprehensive study by Miskelly (2012). Wind droughts occur typically when anticyclones are centered in southern New South Wales, remaining stationary before progressing eastward. Such anticyclone high pressure zones have descending air trending anticlockwise in the southern hemisphere, dispersing outwards. From the vortical action and energy theory described in this article, winds in high pressure zones lack vortical energy at low radius. There may be ways to take advantage of this knowledge in managing power systems. The other challenges to successful adoption of wind power referred to in the Introduction (Elgendi et al., 2023; Thess & Lengsfeld, 2022; Veers et al., 2019; Viré et al., 2022) need the best intellectual research and practice possible for their solution, even if this requires an action revision of the current Bernoulli-based fluid mechanics. Meyers et al. (2022) have pointed out how the complex physics of turbulent flows that we discuss here challenge collective control of arrayed wind turbines. Action mechanics (Kennedy & Hodzic, 2023) replaces the focus on the kinetic energy of wind as the primary source of wind power in favor of the principle of torques as rates of action impulses at varying radii. Commercial success alone is insufficient as a criterion, given the need to consider other important aspects of the local environment.

We emphasize that this article presents a hypothesis that still need rigorous testing. However, for science to advance it is essential that such hypotheses receive due consideration only possible by publication. This testing is even more important in this area critical to renewable energy, climate science, and the successful management of climate.

Supplementary Materials

The following supporting information can be downloaded from website https://doi.org/10.5194/wes-2022-22 or from https://www.ackle.au; Figure S1, Wind power computer program; Table S1, Vevor data output wind angle; Table S2 Vevor data output TSR; Table S3, GE 1.5MW data output; Table S4, Turbine5/Cal Vevor coding; Table S5, AirFoil1/Cal Boeing coding; Table S6, TurbhalT/Cal Twist dataset; Table S7, Python Coding Wind Power plus Mathematica notebook. Supplementary Materials of further information may also be obtained by request from the corresponding author at ivan.kennedy@sydney.edu.au.

Acknowledgments

We are grateful to our host institutions for general support. We thank 10 anonymous reviewers at three journals for helpful comments; all but three reviewers recommended publication, following revisions. We also thank Philip Kuchel at the University of Sydney for physical advice on wind foils and Rafe Champion for years of encouragement regarding the metaphysics of experimentation according to Karl Popper.

Author Contributions

Conceptualization, I.K.; M.H.; and J.R.; methodology, I.K.; M.H.; and N.C.; software, I.K.; and N.C.; validation, M.H.; data curation, I.K.; writing – original draft preparation, I.K.; review and editing, M.H.; I.K.; A.N.C.; and J.R. All authors have read and agreed to the published version of the manuscript.

Funding

This research received no external funding.

Data Availability Statement

All data are given in the article or in Supplementary Materials.

Conflicts of Interest

The authors declare that they have no conflicts of interest to this work.

References

Allen, R. (2005). Penman – Monteith equation. In D. Hillel (Ed.), *Encyclopedia of soils in the environment* (pp. 180–188). Elsevier. https://doi.org/10.1016/B0-12-348530-4/00399-4

Barthelmie, R. J., & Pryor, S. C. (2019). Automated wind turbine wake characterization in complex terrain. *Atmospheric Measurement Techniques*, *12*(6), 3463–3484. https://doi.org/10.5194/amt-12-3463-2019

Batchelor, G. K. (1967). *An introduction to fluid dynamics*. UK: Cambridge University Press.

Businger, S., & Businger, J. A. (2001). Viscous dissipation of turbulence kinetic energy in storms. *Journal of the Atmospheric Sciences*, *58*(24), 3793–3796.

Chakirov, R., & Vagapov, Y. (2011). Direct conversion of wind energy into heat using joule machine. In *2011 International Conference on Environmental and Computer Science, 19,* 12–17.

Chervenkov, S., Wu, X., Bayerl, J., Rohlfes, A., Gantner, T., Zeppenfeld, M., & Rempe, G. (2014). Continuous centrifuge decelerator for polar molecules. *Physical Review Letters*, *112*(1).

Cleugh, H. A. (1998). Effects of windbreaks on airflow, microclimates and crop yields. *Agroforestry Systems*, *41,* 55–84.

Elgendi, M., AlMallahi, M., Abdelkhalig, A., & Selim, M. Y. E. (2023). A review of wind turbines in complex terrain. *International Journal of Thermofluids*, *17*. https://doi.org/10.1016/j.ijft.2023.100289.

Frisch, U. (1995). *Turbulence: The legacy of AN Kolmogorov*. UK: Cambridge University Press.

Geyko, V. I., & Fisch, N. J. (2013). Reduced compressibility and an inverse problem for a spinning gas. *Physical Review Letters*, *110*(15). https://doi.org/10.1103/PhysRevLett.110.150604

Geyko, V. I., & Fisch, N. J. (2016). Piezothermal effect in a spinning gas. *Physical Review E*, *94*(4). https://doi.org/10.1103/PhysRevE.94.042113

Glauert, H. (1935). Airplane propellers. In W. F. Durand (Ed.), *Aerodynamic theory*. Springer.

Harris, R. A., Zhou, L., & Xia, G. (2014). Satellite observations of wind farm impacts on nocturnal land surface temperature in Iowa. *Remote Sensing*, *6*(12), 12234–12246. https://doi.org/10.3390/rs61212234

Johnson, D. A., Gu, M., & Gaunt, B. (2016). Wind turbine performance in controlled conditions: BEM modeling and comparison with experimental results. *International Journal of Rotating Machinery*, *2016*. https://doi.org/10.1155/2016/5460823.

Kennedy, I., Hodzic, M., Crossan, A., Crossan, N., Acharige, N., & Runcie, J. (2022). A new way to estimate maximum power from wind turbines: Linking Newtonian with action mechanics. *Wind Energy Science Discussions*, 1–23. https://doi.org/10.5194/wes-2022-22.

Kennedy, I. R., & Hodzic, M. (2021). Action and entropy in heat engines: An action revision of the Carnot Cycle. *Entropy*, *23*(7), 860. https://doi.org//10.3390/e23070860.

Kennedy, I. R., & Hodzic, M. (2023). Applying the action principle of classical mechanics to the thermodynamics of the troposphere. *Applied Mechanics*, *4*(2), 729–751. https://doi.org/10.3390/applmech4020037

Kennedy, I. R., Hodzic, M., Crossan, A. N., Acharige, N., & Runcie, J. (2021). A new theory for estimating maximum power from wind turbines: A fundamental Newtonian approach. *arXiv preprint: 2110.15117*.

Meyers, J., Bottasso, C., Dykes, K., Fleming, P., Gebraad, P., Giebel, G., . . . , & Van Wingerden, J. W. (2022). Wind farm flow control: Prospects and challenges. *Wind Energy Science Discussions*, *7*(6), 1–56. https://doi.org/10.5194/wes-7-2271-2022.

Miller, L. (2020). The warmth of wind power. *Physics Today*, *73*(8), 58–59. https://doi.org/10.1063/PT.3.4553

Miller, L. M., & Keith, D. W. (2018). Climatic impacts of wind power. *Joule*, *2*(12), 2618–2632.

Miskelly, P. (2012). Wind farms in eastern Australia—Recent lessons. *Energy & Environment*, *23*(8), 1233–1260.

Navaz, H. K., Chan, E., & Markicevic, B. (2008). Convective evaporation model of sessile droplets in a turbulent flow—Comparison with wind tunnel data. *International Journal of Thermal Sciences*, *47*(8), 963–971. https://doi.org/10.1016/j.ijthermalsci.2007.08.004

Nygaard, N. G. (2014). Wakes in very large wind farms and the effect of neighbouring wind farms. *Journal of Physics: Conference Series*, *524*(1).

Platis, A., Siedersleben, S. K., Bange, J., Lampert, A., Bärfuss, K., Hankers, R., . . . , & Emeis, S. (2018). First in situ evidence of wakes in the far field behind offshore wind farms. *Scientific Reports*, *8*(1), 2163. https://doi.org/10.1038/s41598-018-20389-y.

Regis, E. (2020). The enigma of aerodynamic lift. *Scientific American*, *322*(2), 44–51.

Roy, S. B., & Traiteur, J. J. (2010). Impacts of wind farms on surface air temperatures. In *Proceedings of the National Academy of Sciences*, *107*(42), 17899–17904. https://doi.org/10.1073/pnas.1000493107

Schubel, P. J., & Crossley, R. J. (2012). Wind turbine blade design. *Energies*, *5*(9), 3425–3449. https://doi.org/10.3390/en5093425.

Sørensen, J. N. (2016). *General momentum theory for horizontal axis wind turbines*. In J. Peinke & G. van Bussel (Eds.), *Research Topics in Wind Energy*. Springer Cham.

Thess, A. D., & Lengsfeld, P. (2022). Side effects of wind energy: Review of three topics—Status and open questions. *Sustainability*, *14*(23). https://doi.org/10.3390/su142316186.

Veers, P., Dykes, K., Lantz, E., Barth, S., Bottasso, C. L., Carlson, O., . . . , & Wiser, R. (2019). Grand challenges in the science of wind energy. *Science*, *366*(6464). https:///www.science.org/doi/10.1126/science.aau2027.

Viré, A., LeBlanc, B., Steiner, J., & Timmer, N. (2022). Experimental study of the effect of a slat on the aerodynamic performance of a thick base airfoil. *Wind Energy Science*, *7*(2), 573–584. https://doi.org/10.5194/wes-7-573-2022.

Wang, G., Li, G., & Liu, Z. (2023). Wind farms dry surface soil in temporal and spatial variation. *MethodsX*, *10*. https://doi.org/10.1016/j.mex.2023.102000.

Zhu, W. J., Shen, W. Z., & Sørensen, J. N. (2014). Integrated airfoil and blade design method for large wind turbines. *Renewable Energy*, *70,* 172–183. http://dx.doi.org/10.1016/j.renene.2014.02.057.

How to Cite: Kennedy, I. R., Hodzic, M., Crossan, A. N., Crossan, N., Acharige, N., & Runcie, J. W. (2023). Estimating Maximum Power from Wind Turbines with a Simple Newtonian Approach. *Archives of Advanced Engineering Science* 1(1), 38–54, https://doi.org/10.47852/bonviewAAES32021330